

The Ideal Glass and the Ideal Disk Packing in Two Dimensions

Viola M. Bolton-Lum,¹ R. Cameron Dennis,^{2,3} Peter Morse,⁴ and Eric Corwin¹

¹*Department of Physics and Materials Science Institute,
University of Oregon, Eugene, Oregon 97403, USA.*

²*Department of Physics and Astronomy, University of Pennsylvania,
209 South 33rd Street, Philadelphia, Pennsylvania 19104, USA*

³*Department of Physics and Soft Matter Program,
Syracuse University, Syracuse, New York 13244, USA*

⁴*Department of Chemistry, Department of Physics and Princeton Institute of Materials,
Princeton University, Princeton, New Jersey 08544, USA*

(Dated: April 12, 2024)

The ideal glass, a disordered system of particles with zero configurational entropy, cannot be realized through thermal processes. Nevertheless, we present a method for constructing ideal jammed packings of soft spheres, and thus the zero temperature ideal glass, in two dimensions. In line with the predicted properties, these critically jammed packings have high bulk and shear moduli as well as an anomalously high density. While the absence of pressure scaling in the shear moduli of crystalline materials is often attributed to the ordered nature of the particles, we show for the first time that disordered ideal packings also have this feature. We also find that the density of states avoids the low frequency power law scaling famously found in most amorphous materials. Finally, these configurations display hyperuniformity. In addition to resolving a long-standing mystery, this methodology represents a valuable shortcut in the generation of well-equilibrated glassy systems. The creation of such an ideal packing makes possible a complete exploration and explanation of two dimensional jammed and glassy systems.

Introduction – Glasses and jammed packings are disordered systems characterized by diverging relaxation timescales and rough energy landscapes [1–3]. Poorly annealed glasses display non-phononic densities of states [4] and small Poisson ratios in the low pressure limit. Well annealed or “ultrastable” glasses tend towards greater Poisson ratios and increased thermal stability but require extensive aging or additional degrees of freedom during formation. Additional degrees of freedom have been implemented both experimentally [5–8] and computationally [9–18] to produce ultrastable glasses and jammed systems efficiently. The theoretical “ideal glass” bounds ultrastability; it is an equilibrium super-cooled liquid with configurational entropy that is a global minimum and thus equal to that of the crystal [8, 19]. For sphere packings this corresponds to a global maximum of density at zero pressure. However, the timescales required to achieve an ideal glass through the equilibrium cooling of a liquid are necessarily infinite [3, 20–22], seemingly forbidding the creation of an ideal glass. Here, we show a non-equilibrium mechanism for creating a two-dimensional ideal glass of polydisperse disks at zero temperature, which can also be termed an ideal jammed packing. This mechanism satisfies our proposed definition of an ideal jammed packing as 1) having a fully triangulated contact network, 2) lacking long range orientational and translational order, 3) mechanically ultrastable, 4) hyperuniform, and 5) having an anomalously high melting temperature, equal to the Kauzmann temperature. The creation of such an ideal packing makes possible a complete exploration and explanation of two dimensional jammed and glassy systems.

Packing Protocols – A system of N disks in 2-dimensions has $2N$ translational degrees of freedom. At jamming, every degree of freedom is constrained, and thus the system must have $2N$ contacts between disks [23, 24]. Since every contact is shared by two disks each disk must then have an average coordination number of 4. A triangulated packing, by contrast, must have an average coordination number of 6 [25]. We achieve this by adding an additional degree of freedom to every disk in the form of a mutable radius.

The following protocol employs radii degrees of freedom to construct fully coordinated ideal amorphous packings in two dimensions while approximately preserving an input distribution of radii. This protocol builds on the use of transient degrees of freedom [14] and conformal circle packing [25, 26].

Triangulated packings – N disks are uniformly randomly placed into a square simulation box with side length 1 and periodic boundary conditions. Disks are assigned radii drawn from a log-normal distribution with 20% polydispersity, chosen to avoid crystallization [27]. Radii are scaled to an initial packing fraction $\varphi = 0.915$, chosen to result in highly coordinated (i.e. hyperstatic) packings [28, 29]. Particles interact through the soft sphere harmonic interaction potential

$$U = \sum_{\langle ij \rangle} \frac{1}{2} \left(1 - \frac{r_{ij}}{\sigma_{ij}} \right)^2 \Theta \left(1 - \frac{r_{ij}}{\sigma_{ij}} \right), \quad (1)$$

where the sum is over pairs of indices $\langle ij \rangle$, σ_{ij} is the sum of the i th and j th radii and r_{ij} is the distance between centers. We use PyCudaPacking [30, 31], a GPU based

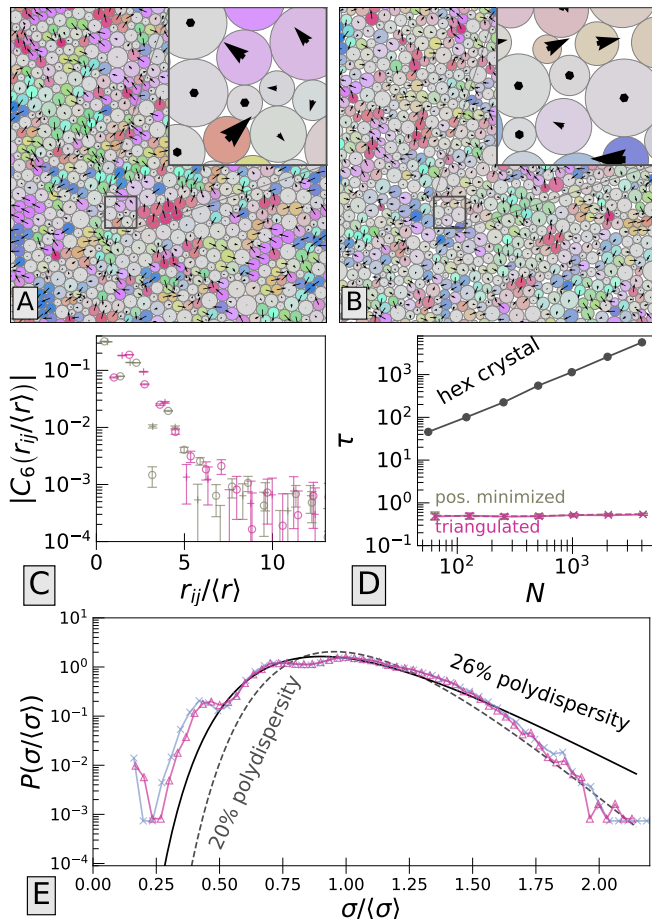


FIG. 1. a) Triangulated packing, and b) conventionally jammed packing with $N = 1024$ and an identical set of radii. The crystalline order parameter ψ_6 is indicated by face color and overlaid vectors. c) The orientational correlation function, C_6 , for triangulated packings (magenta) and conventionally jammed packings (gray). d) The finite size scaling of the translational order parameter, τ , for triangulated packings (magenta), conventionally jammed packings (gray), and the hexagonal crystal (black). e) The probability distribution of disk diameters, $P(\sigma)/(\sigma)$ averaged over 10 packings of 4096 disks. The starting distribution is at 20 % polydispersity (gray dashed line), the distribution after radii-minimization is plotted as gray x's, the distribution after triangulation is plotted as magenta triangles, and for comparison a 26 % polydisperse distribution is shown in black.

software package with an implementation of the FIRE algorithm [32], to adjust the positions and radii of the disks to find the inherent state structure, a local minimum of energy. Similarly to Hagh *et al.* [14], the radii degrees of freedom are subject to constraints on moments of the radius distribution, in order to avoid falling into various trivial global minima. The result of such a minimization is nearly triangulated, however these additional constraints necessarily introduce at least an equal number of “defects” into our system in the form of missing

contacts.

To produce fully triangulated jammed packings we employ CirclePack [25] to produce a new disk packing from the radical Delaunay triangulation. CirclePack produces configurations of particle positions and radii in orthorhombic periodic boundary conditions such that each particle is tangent to all of its Delaunay neighbors. CirclePack can be seen as relaxing away the “defects” in the original disk packing, leading to a triangulated and critically jammed packing. Our protocol yields packings at jamming fraction $\varphi \simeq 0.910$, the densest such 2d amorphous packings of which we are aware. Further, this density is meaningfully larger than that of the size-segregated hexagonal lattice of disks, $\varphi_{\text{hex}} = \pi/\sqrt{12} \approx 0.9069$, and much larger than the typical jamming density for conventionally prepared packings with the same disk size distributions as the triangulated packings, $\varphi_J \simeq 0.849$ [28, 29].

This process leaves the radii distribution approximately fixed relative to the radii minimized packings. Figure 1 shows that triangulated packings with initial radii drawn from a 20 % polydispersity log normal distribution are distributed more closely to a 26 % polydisperse log normal distribution after radii minimization. The final step of creating the perfectly triangulated packing typically involves changes to particles relative radii on the order of 0.2 %. Triangulated packings are illustrated in Figure 1a.

We subsequently produce packings at a range of pressures by increasing the packing fraction as guided by the protocol described in [30].

From each triangulated packing we produce conventionally jammed position-minimized packings with identical radii distributions by randomizing positions and then minimizing energy with respect to only position degrees of freedom [33]. Conventionally jammed packings are illustrated in Figure 1b.

Properties of an Ideal Packing – We demonstrate that our triangulated packings meet all of the requirements for an ideal jammed packing:

1) Ideal packings must be triangulated. A non-triangulated packing will necessarily and generically have neighboring particles which are separated by small gaps. Relaxing those gaps away must then lead to a denser packing. By construction, triangulated packings have a fully triangulated contact network.

2) Ideal amorphous packings must, by definition, have no orientational or translational order. We demonstrate this lack in triangulated packings by computing the correlation function of the orientational order parameter ψ_6 [34], and the finite size scaling of the of the translational order metric τ [35].

The local orientational order parameter, $\psi_{6,i}$, for disk

i is defined as,

$$\psi_{6,i} = \frac{1}{N} \sum_{j=1}^{N_i} e^{6\theta_{ij}}, \quad (2)$$

where N_i is the number of neighbors, θ_{ij} is the polar angle of the vector between particle i and neighbor j [34]. The correlation function $C_6(r)$

$$C_6(r) = \langle \psi_6(\vec{r}_1) \psi_6^*(\vec{r}_2) \rangle_{|\vec{r}_2 - \vec{r}_1| = r}, \quad (3)$$

an average over ψ_6 pairs separated by distance r , is constant for a crystal but decays exponentially for both the conventionally jammed and triangulated packings amorphous systems, as shown in Figure 1d.

The translational order metric τ [35], is defined in 2D space as

$$\frac{1}{D^2} \int (g(r) - 1)^2 d\vec{r}, \quad (4)$$

where $g(r)$ is the pair correlation function and D is a length scale chosen to be the average particle radius. Finite size scaling in τ indicates the degree of long range translational order in a system; Poisson distributed points have $\tau = 0$ for all system sizes, amorphous disk packings maintain a constant non-zero value of τ with increasing N , and ordered systems show power law growth in τ with N . Figure 1d shows τ as a function of system size for the hexagonal crystal (circles), conventionally jammed systems (in gray, labelled), and triangulated packings (violet, labelled).

Taken together, these two measurements demonstrate that triangulated packings are equally amorphous as conventionally jammed packings.

3) Ideal packings must be mechanically ultrastable as a result of being the deepest well in the energy landscape. Ideal jammed packings must be strictly jammed, in the sense that no collective motions or strains lead to unjamming motions [36–39]. We know from the Maxwell-Calladine index theorem [23, 40] that conventionally jammed packings at zero pressure cannot be strictly jammed since floppy modes must exist which correspond to collective motions of the particles and the boundaries which do not cause particle overlaps. These collective motions come at no energy cost which means they are associated with a zero shear modulus in that direction. Having more contacts than position and strain degrees of freedom is thus a necessary, but not sufficient, condition for strict jamming. By employing a linear programming algorithm [36, 38] that takes into consideration the one-sided contact potential, we find that all triangulated packings tested up to $N = 4096$ are strictly jammed, and thus members of a significantly more stringent class of stability that is typically reserved for crystalline systems.

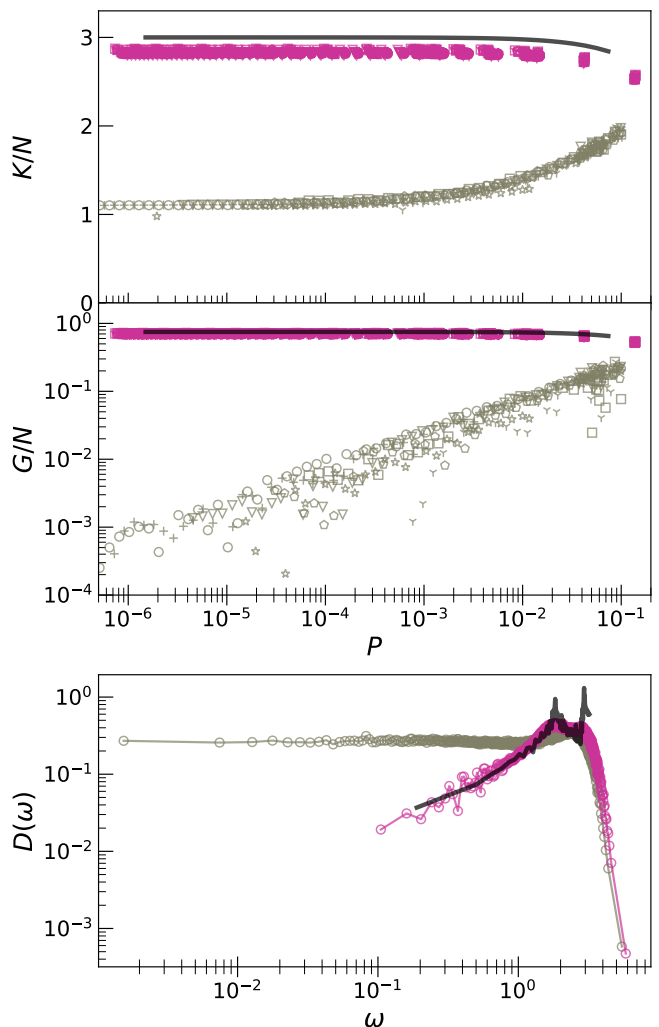


FIG. 2. top) Bulk modulus per particle, K/N is plotted as a function of pressure, P for triangulated packings (magenta), conventionally jammed packings (gray), and hexagonal crystals for N ranging from 64 to 4096 in powers of two (indicated by different symbols). Conventionally jammed packings are averaged over 10 independent packings while triangulated packings are displayed without averaging. middle) Shear modulus per particle, G/N , are presented with the same colors and symbols. bottom) Density of vibrational states, $D(\omega)$, are presented with the same colors and symbols; only $N = 4096$ is shown for clarity.

Figure 2 shows the mechanical properties of conventional, triangulated packings, and the hexagonal crystal. We calculate elastic moduli [41] and the vibrational density of states using the linear dynamical matrix of a packing. Triangulated packings are mechanically ultrastable as indicated by constant, and anomalously large, bulk and shear moduli as pressure is brought to zero, in contrast to the vanishing shear modulus at zero pressure found in conventionally jammed packings. Further, they play host to vibrational modes at vanishing pressure which are governed by the Debye, or Phononic [8, 42],

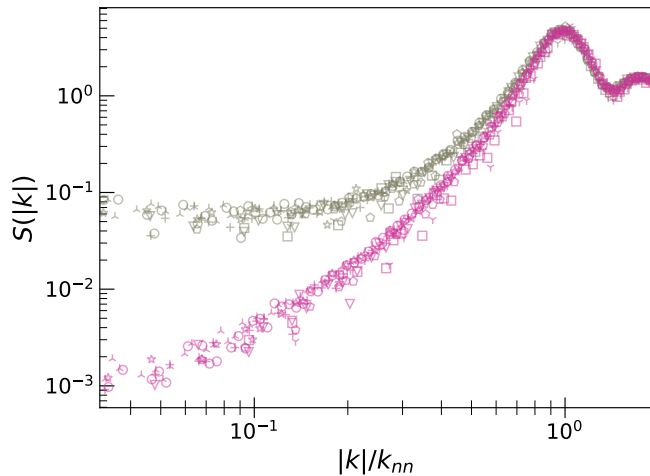


FIG. 3. Averages over histograms of discrete Fourier transforms of point densities, scaled by \sqrt{N} to collapse curves from $N = 64 - 4096$. N is indicated by choice of marker. Color indicates protocol; gray for position-minimized packings and magenta for triangulated packings.

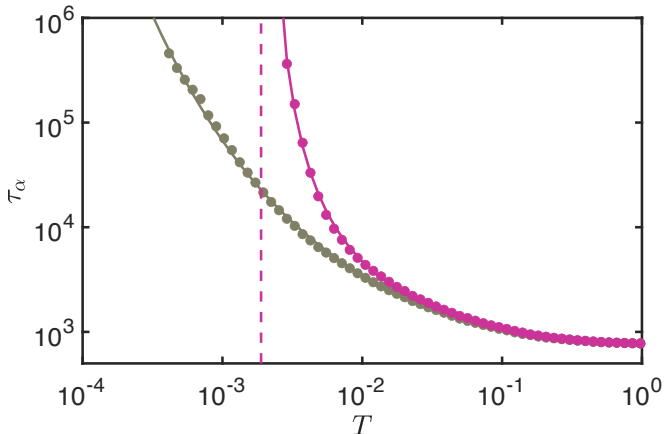


FIG. 4. Measurements of the relaxation time for a sample triangulated packing (magenta) and conventionally jammed packing (gray), each with $N = 8192$ using 10 thermal averages. Fits are to the modified VFT form of Eq. (7), and the divergence in the triangulated packing at $T_m = 0.00189(10)$ is shown as a dashed line.

scaling of crystals and ultrastable systems and lack the Boson peak [2, 43] of conventionally jammed packings. In sum, the mechanical properties of triangulated packings are much more similar to those of crystals than to those of conventionally jammed packings.

4) An ideal packing must have vanishing long range density fluctuations and thus be hyperuniform [44]. If it had such fluctuations then one could cut out the lower density regions and replace them with copies of the higher density regions in order to achieve a denser packing. We show that our triangulated packings are hyperuniform by directly measuring the long wavelength (and thus small

wavenumber, \vec{k}) scaling in the static structure factor for weighted points, defined as:

$$S(\vec{k}) = \frac{1}{N} \rho(\vec{k}) \rho(-\vec{k}), \quad (5)$$

where

$$\rho(\vec{k}) = \frac{1}{\langle r^d \rangle} \sum_{j=1}^N r_j^d e^{i\vec{k} \cdot \vec{x}_j}. \quad (6)$$

We take a Fourier space angular average to produce $S(|k|)$ [45], which is shown in Figure 3 for conventional and triangulated packings.

Hyperuniformity, the suppression of long range density fluctuations, corresponds to a vanishing value of $S(|k|)$ in the limit of small $|k|$ [44, 46]. We note a plateau in $S(|k|)$ for position-minimized packings. By contrast, triangulated packings show approximately power law behavior for small k [47–49].

5) The melting temperature measures the thermodynamic stability of a glass and encodes information about the height of the barriers about the stable basin. In an ideal glass the melting temperature should be higher than that of any other glass and equal to the Kauzmann temperature. To measure the melting temperature, we apply simple Monte Carlo dynamics at a range of temperatures T and measure the associated α -relaxation time, τ_α [50]. The melting temperature T_m is then extracted from a fit to the modified Vogel-Fulcher-Tammann (VFT) form [51].

$$\tau_\alpha = \tau_0 \exp \left[\frac{DT_m}{(T - T_m)^c} \right] \quad (7)$$

where D is the diffusion constant and c is an exponent indicating the ductility of the glass, with higher values of c indicating stronger glasses [1]. We perform 10 thermal averages on each sample, average the values of τ_α , and perform a fit to determine T_m . We find that the conventional packings have $T_m < 10^{-6}$, while the triangulated packings have a melting temperature many orders of magnitude larger, $T_m = 0.0019(2)$ with the error bar indicating sample to sample variation. While in principle this should correspond to a Kauzmann temperature, its existence in 2-dimensions has been debated [52].

Conclusion – The nature of the glass transition remains a mystery, but the question of whether an ideal configuration exists lies at the heart of this mystery [20]. The constructive scheme presented herein demonstrates not only that ideal packings exist but that they have superlative structural, mechanical, and thermal properties. This represents a leap forward in understanding the complex energy landscapes underlying disordered systems and places the existence of a thermodynamic glass phase on firm footing. By working backwards from the ideal system through the introduction of defects we can hope

to fully explore the glassy landscape of two-dimensional amorphous systems. Ideal packings are not just interesting from a theoretical perspective, but from a practical one as well. Such packings are fully amorphous while presenting the bulk material and thermal properties of crystalline materials: ultrastability, hyperuniformity, and a high melting temperatures; all properties that are desirable from an industrial perspective.

Acknowledgements – We thank Francesco Arceri, Ludovic Berthier, Varda Hagh, and Sascha Hilgenfeldt for valuable discussions. This work benefited from access to the University of Oregon high performance computer, Talapas. This work was supported by the Simons Foundation No. 454939 (V.B.L., R.C.D, and E.I.C.).

-
- [1] P. G. Debenedetti and F. H. Stillinger, *Nature* **410**, 259 (2001).
- [2] M. L. Manning and A. J. Liu, *EPL (Europhysics Letters)* **109**, 36002 (2015).
- [3] P. Charbonneau, J. Kurchan, G. Parisi, P. Urbani, and F. Zamponi, *Annual Review of Condensed Matter Physics* **8**, 265 (2017).
- [4] K. Shiraishi, H. Mizuno, and A. Ikeda, “Non-phononic density of states of two-dimensional glasses revealed by random pinning,” (2023), arXiv:2301.06225 [cond-mat].
- [5] L. Berthier, G. Biroli, P. Charbonneau, E. I. Corwin, S. Franz, and F. Zamponi, *The Journal of Chemical Physics* **151**, 010901 (2019).
- [6] C. Rodriguez-Tinoco, M. Gonzalez-Silveira, M. A. Ramos, and J. Rodriguez-Viejo, *La Rivista del Nuovo Cimento* **45**, 325 (2022).
- [7] M. D. Ediger, *The Journal of Chemical Physics* **147**, 210901 (2017).
- [8] C. P. Royall, F. Turci, S. Tatsumi, J. Russo, and J. Robinson, *Journal of Physics: Condensed Matter* **30**, 363001 (2018).
- [9] D. Gazzillo and G. Pastore, *Chemical Physics Letters* **159**, 388 (1989).
- [10] S. Kim and S. Hilgenfeldt, *Physical Review Letters* **129**, 168001 (2022).
- [11] F. Ghimenti, L. Berthier, and F. van Wijland, “Irreversible Monte Carlo algorithms for hard disk glasses: from event-chain to collective swaps,” (2024), arXiv:2402.06585 [cond-mat].
- [12] S. Kim and S. Hilgenfeldt, (2024), 10.48550/ARXIV.2402.08390.
- [13] G. Kapteijns, W. Ji, C. Brito, M. Wyart, and E. Lerner, *Physical Review E* **99**, 012106 (2019).
- [14] V. F. Hagh, S. R. Nagel, A. J. Liu, M. L. Manning, and E. I. Corwin, *Proceedings of the National Academy of Sciences* **119**, e2117622119 (2022).
- [15] L. Berthier, D. Coslovich, A. Ninarello, and M. Ozawa, *Physical Review Letters* **116**, 238002 (2016).
- [16] A. Ninarello, L. Berthier, and D. Coslovich, *Physical Review X* **7**, 021039 (2017).
- [17] G. Szamel, *Physical Review E* **98**, 050601 (2018).
- [18] H. Ikeda, F. Zamponi, and A. Ikeda, *The Journal of Chemical Physics* **147**, 234506 (2017).
- [19] W. Kauzmann, *Chemical Reviews* **43**, 219 (1948).
- [20] L. Berthier and G. Biroli, *Reviews of Modern Physics* **83**, 587 (2011).
- [21] G. Parisi and F. Zamponi, *Reviews of Modern Physics* **82**, 789 (2010).
- [22] P. Charbonneau, Y. Jin, G. Parisi, and F. Zamponi, *Proceedings of the National Academy of Sciences* **111**, 15025 (2014).
- [23] J. C. Maxwell, *The London, Edinburgh, and Dublin Philosophical Magazine and Journal of Science* **27**, 294 (1864).
- [24] V. F. Hagh and M. F. Thorpe, *Physical Review B* **98**, 100101 (2018).
- [25] K. Stephenson, *Introduction to Circle Packing: the Theory of Discrete Analytic Functions* (Cambridge University Press, New York, 2005).
- [26] G. L. Orick, K. Stephenson, and C. Collins, *Computational Geometry* **64**, 13 (2017).
- [27] H. Tong, P. Tan, and N. Xu, *Scientific Reports* **5**, 15378 (2015).
- [28] C. S. O’Hern, S. A. Langer, A. J. Liu, and S. R. Nagel, *Physical Review Letters* **88**, 075507 (2002).
- [29] C. S. O’Hern, L. E. Silbert, A. J. Liu, and S. R. Nagel, *Physical Review E* **68**, 011306 (2003).
- [30] P. Charbonneau, E. I. Corwin, G. Parisi, and F. Zamponi, *Physical Review Letters* **114**, 125504 (2015).
- [31] P. K. Morse and E. I. Corwin, *Physical Review Letters* **112**, 115701 (2014).
- [32] E. Bitzek, P. Koskinen, F. Gähler, M. Moseler, and P. Gumbsch, *Physical Review Letters* **97**, 170201 (2006).
- [33] P. Charbonneau, E. I. Corwin, G. Parisi, and F. Zamponi, *Physical Review Letters* **109**, 205501 (2012).
- [34] B. I. Halperin and D. R. Nelson, *Physical Review Letters* **41**, 121 (1978).
- [35] S. Torquato, G. Zhang, and F. Stillinger, *Physical Review X* **5**, 021020 (2015).
- [36] A. Donev, S. Torquato, F. H. Stillinger, and R. Connelly, *Journal of Computational Physics* **197**, 139 (2004).
- [37] R. Connelly, *European Journal of Combinatorics* **29**, 1862 (2008).
- [38] A. Donev, S. Torquato, F. H. Stillinger, and R. Connelly, *Journal of Applied Physics* **95**, 989 (2004).
- [39] S. Torquato and F. H. Stillinger, *Journal of Applied Physics* **102**, 093511 (2007).
- [40] C. R. Calladine, *International Journal of Solids and Structures* **14**, 161 (1978).
- [41] R. Dennis and E. Corwin, *Physical Review Letters* **128**, 018002 (2022).
- [42] D. Xu, S. Zhang, H. Tong, L. Wang, and N. Xu, *Nature Communications* **15**, 1424 (2024).
- [43] P. Charbonneau, E. I. Corwin, G. Parisi, A. Poncet, and F. Zamponi, *Physical Review Letters* **117**, 045503 (2016).
- [44] S. Torquato and F. H. Stillinger, *Physical Review E* **68**, 041113 (2003).
- [45] J. R. Dale, J. D. Sartor, R. C. Dennis, and E. I. Corwin, *Physical Review E* **106**, 024903 (2022).
- [46] S. Torquato, *Physics Reports* **745**, 1 (2018).
- [47] M. Skoge, A. Donev, F. H. Stillinger, and S. Torquato, *Physical Review E* **74**, 041127 (2006).
- [48] E. Tjhung and L. Berthier, *Physical Review Letters* **114**, 148301 (2015).
- [49] A. Ikeda, L. Berthier, and G. Parisi, *Physical Review E* **95**, 052125 (2017).
- [50] D. Frenkel and B. Smit, *Understanding Molecular Simu-*

- lation: from Algorithms to Applications*, 2nd ed., Computational science series No. 1 (Academic Press, San Diego, 2002).
- [51] L. S. Garcia-Colin, L. F. Del Castillo, and P. Goldstein, Physical Review B **40**, 7040 (1989).
- [52] L. Berthier, P. Charbonneau, A. Ninarello, M. Ozawa, and S. Yaida, Nature Communications **10**, 1508 (2019).